Origin of eclipsing time variations in post-common-envelope binaries

Prof. Dominik Schleicher
Department of Physics
Sapienza University of Rome

Collaborators:
Robi Banerjee (Hamburg), juan Pablo Hidalgo (Rome), **Felipe Navarrete** (Barcelona/Hamburg), Petri Kapyla (Freiburg), Carolina Ortiz (Hamburg), Barbara Toro (Concepcion), Marcel Voelschow (Hamburg)

Formation of Post-Common-Envelope Binaries: The common envelope phase

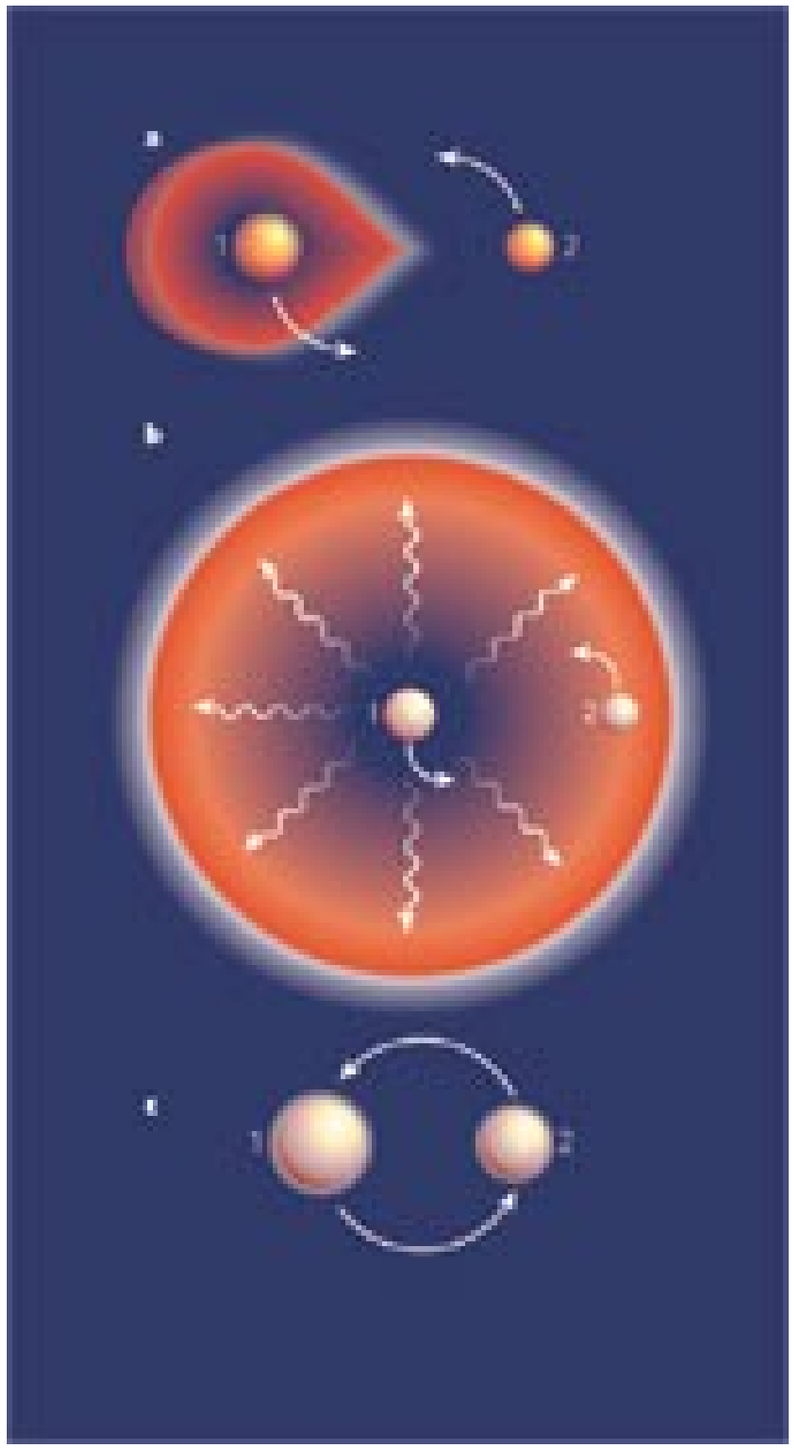

Companion looses angular momentum due to tidal forces -> plunge into the envelope.

Dynamical friction-> companion spirals into center ofgiant, energy deposition.

Gas expelled via energy deposition,companion orbits core of the giant.

Core evolves into White Dwarf.

Eclipsing time variations in NN Ser

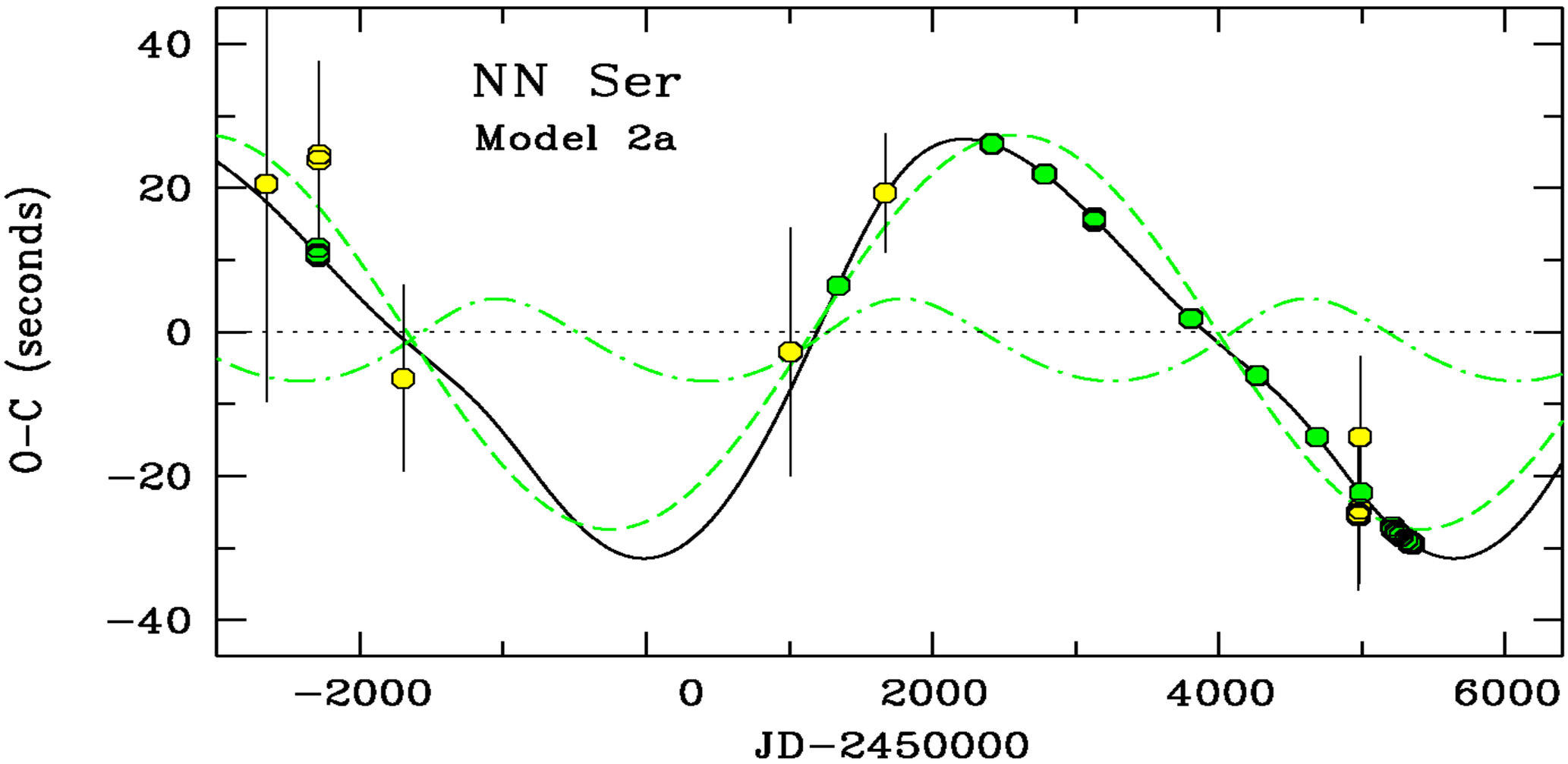

Beuermann et al. (2010, 2013)

The light travel time effect

Eclipsing binaries are oriented to the observer such that both stars regularly overlap.

The overlap leads to periodic variations in the observed magnitude.

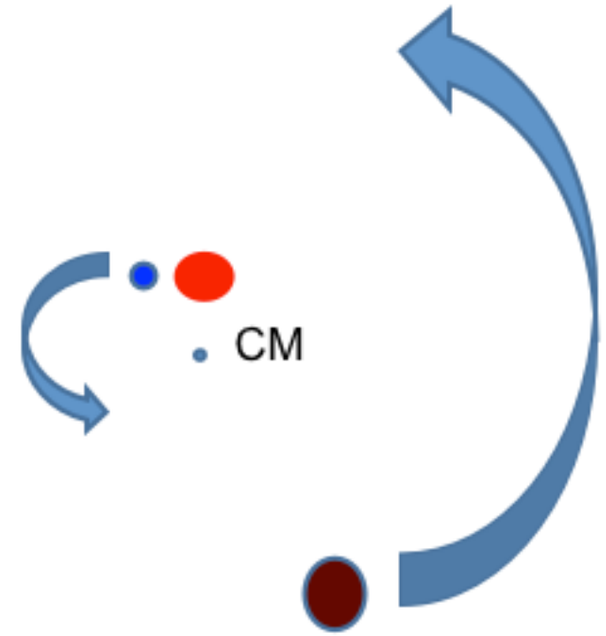

In the presence of a planet the center of mass shifts towards the planet.

Depending on the properties of the planetary orbit, a second signal with the period of the planetary orbit is modulated onto the eclipses.

Potential explanation: Planets in NN Ser

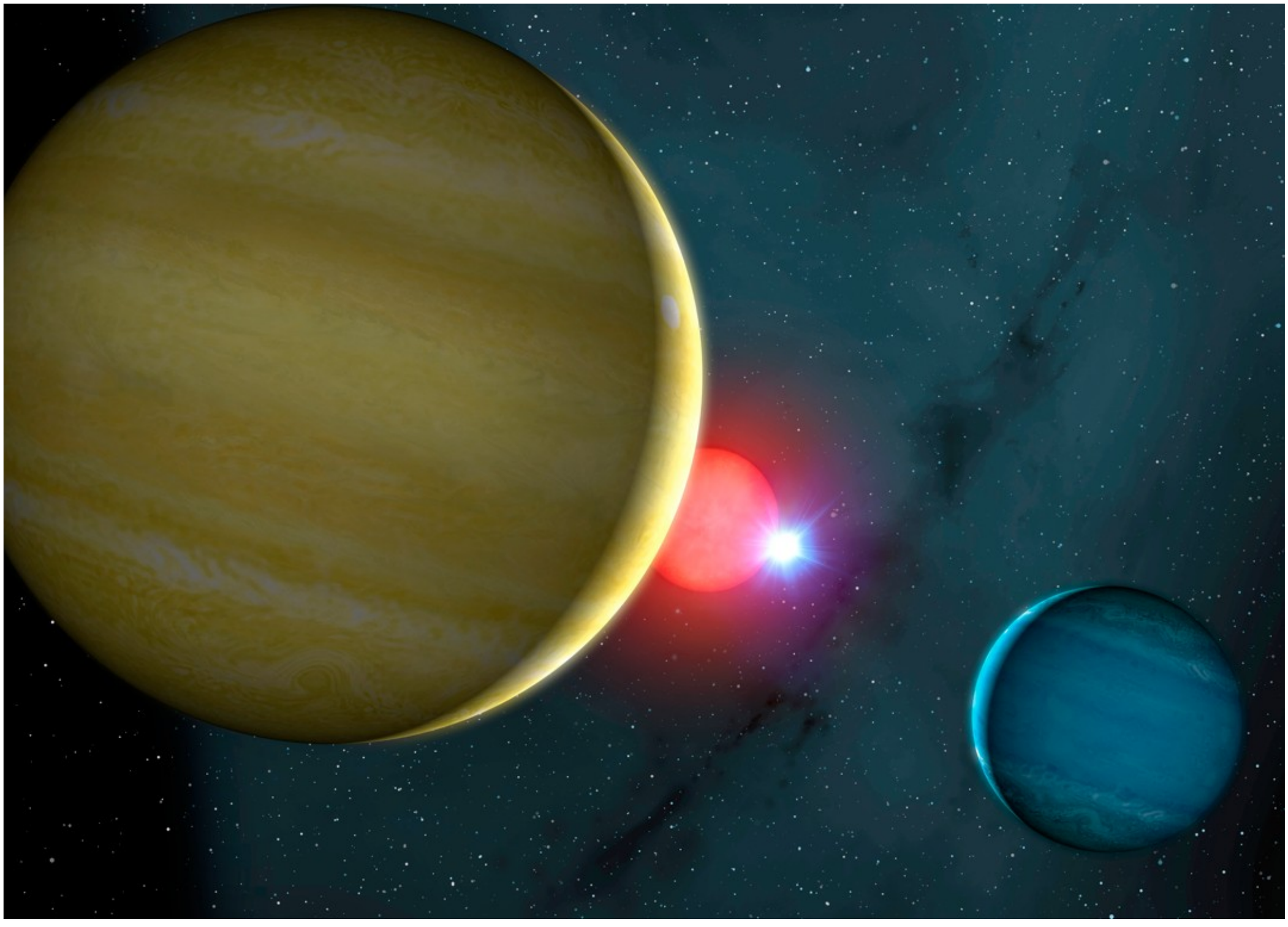

Eclipsing time variations in other PCEBs

Name	$M \sin(i)$ [Mj]	P [yr]	$a \sin(i)$ [AU]	e	Ref.	Notes
HW Vir c	14.3 ± 1.0	12.7 ± 0.2	4.69 ± 0.06	0.40 ± 0.10	1	
HW Vir d	30–120	55 ± 15	12.8 ± 0.2	0.05:	1	*
HS0705+6700 c	31.5 ± 1.0	8.41 ± 0.05	3.52	0.38 ± 0.05	2	*
HS2231+2441 c	13.94 ± 2.20	15.7	~5.16	–	3	
NSVS14256825 c	2.8 ± 0.3	3.49 ± 0.21	1.9 ± 0.3	0.00 ± 0.08	4	
NSVS14256825 d	8.0 ± 0.8	6.86 ± 0.25	2.9 ± 0.6	0.52 ± 0.06	4	
NY Vir c	2.3 ± 0.3	7.9	3.3 ± 0.8	–	5	
NY Vir d	2.5:	>15	≳5.08	–	5	
NN Ser c	6.91 ± 0.54	15.50 ± 0.45	5.38 ± 0.20	0.0	6	
NN Ser d	2.28 ± 0.38	7.75 ± 0.35	3.39 ± 0.10	0.20 ± 0.02	6	
V471 Tau c	46-111	33.2 ± 0.2	~12.6–12.8	0.26 ± 0.02	7	*
QS Vir c	9.01	14.4	~6.32	0.62	8	
QS Vir d	56.59	16.99	~7.15	0.92	8	*
RR Cae c	4.2 ± 0.4	11.9 ± 0.1	5.3 ± 0.6	0	9	
UZ For c	6.3 ± 1.5	16+3	5.9 ± 1.4	0.04 ± 0.05	10	
UZ For d	7.7 ± 1.2	5.25 ± 0.25	2.8 ± 0.5	0.05 ± 0.05	10	
HU Aqr c	7.1	9.00 ± 0.05	4.30	0.13 ± 0.04	11	
DP Leo c	6.05 ± 0.47	28.01 ± 2.00	8.19 ± 0.39	0.39 ± 0.13	12	

Zorotovic & Schreiber (2013)
* indicates Brown Dwarf rather than planet

Problems with planetary interpretation

In some systems, current data require up to 3 planets and/or additional quadratic terms to explain the variations.

In some systems, the proposed planets are dynamically unstable, or the planetary orbits are relatively exotic, including retrograde orbits.

Direct imaging in V 471 Tau did not reveal a planet (Hardy et al. 2015).

Alternative: Magnetic activity

Magnetic fields induce quasi-periodic changes in the stellar quadrupole moment Q, leading to the observed eclipsing time variations.

Applegate (1992): Thin-shell model requires

$$\Delta Q = -\frac{\Delta P}{P} \cdot \frac{a_{bin}^2 M_{sec}}{9}$$

Change in angular momentum: $\Delta J = \frac{G M_{\rm sec}^2}{R_{\rm sec}} \left(\frac{a_{\rm bin}}{R_{\rm sec}} \right)^2 \frac{\Delta P}{6\pi}$

Energy to transfer the angular momentum:

$$\Delta E = \Omega_{\rm dr} \Delta J + \frac{(\Delta J)^2}{2 I_{\rm eff}}$$

A finite-shell model for the quadrupole moment

Angular momentum conservation:

$$I_1 \Delta\Omega_1 + I_2 \Delta\Omega_2 = 0$$

Amount of differential rotation: $\Omega_{\mathrm{dr}} = \Omega_2 - \Omega_1$

Relation between the change of angular velocity and quadrupole moment:

$$\Delta Q = Q_1' \left[2\Omega_1 \Delta\Omega_1 + (\Delta\Omega_1)^2 \right] + Q_2' \left[2\Omega_2 \Delta\Omega_2 + (\Delta\Omega_2)^2 \right]$$

Required energy to change the structure:

$$\Delta E = \Omega_{\mathrm{dr}} \Delta J + \frac{1}{2} \left(\frac{1}{I_1} + \frac{1}{I_2} \right) (\Delta J)^2$$

Brinkworth et al. (2006)

Application to NN Ser

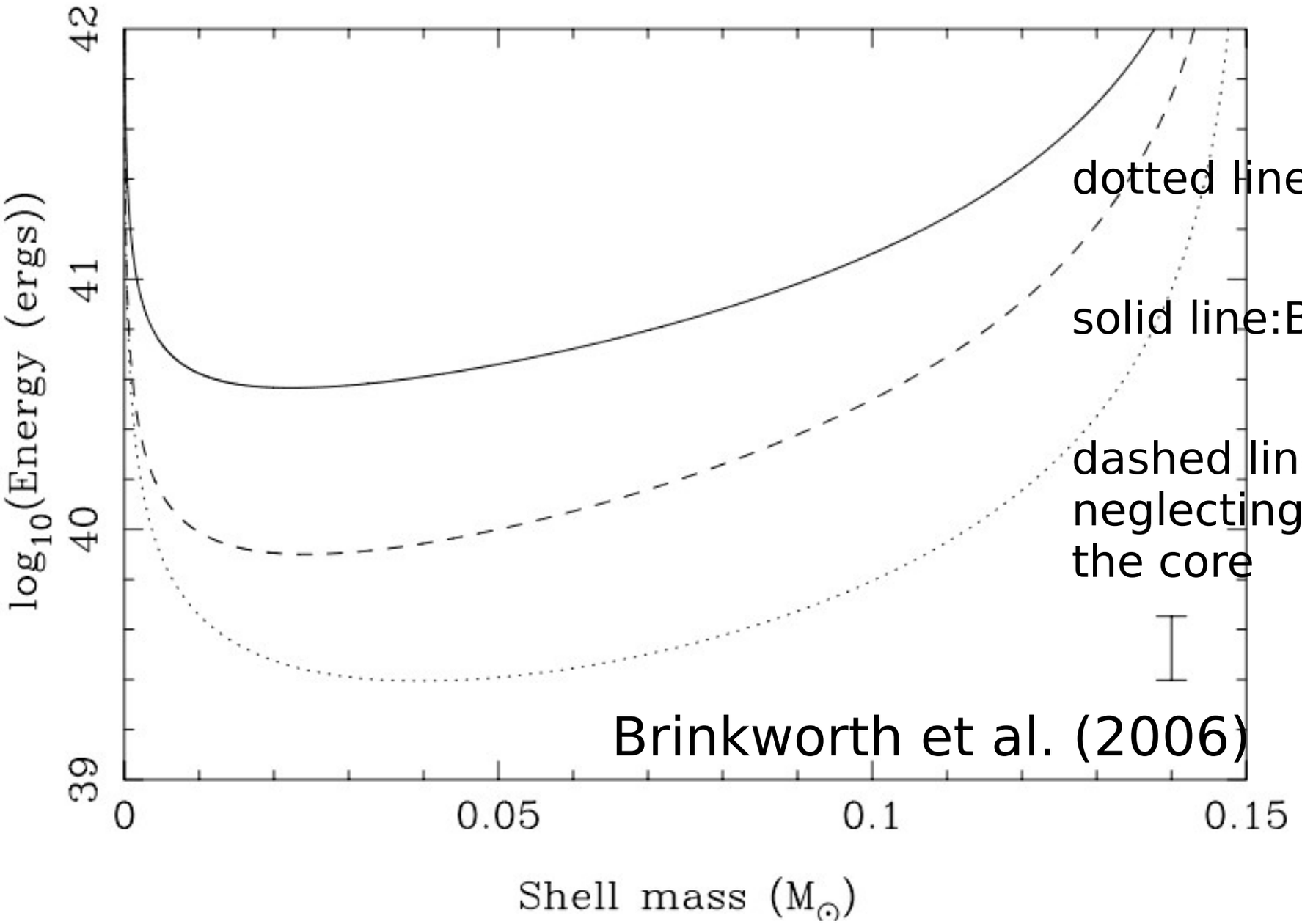

Available energy over 15 years:

$$2.5 \times 10^{39} \leqslant E_2 \leqslant 4.5 \times 10^{39}\,\mathrm{erg}$$

Required energy depends on binary configuration

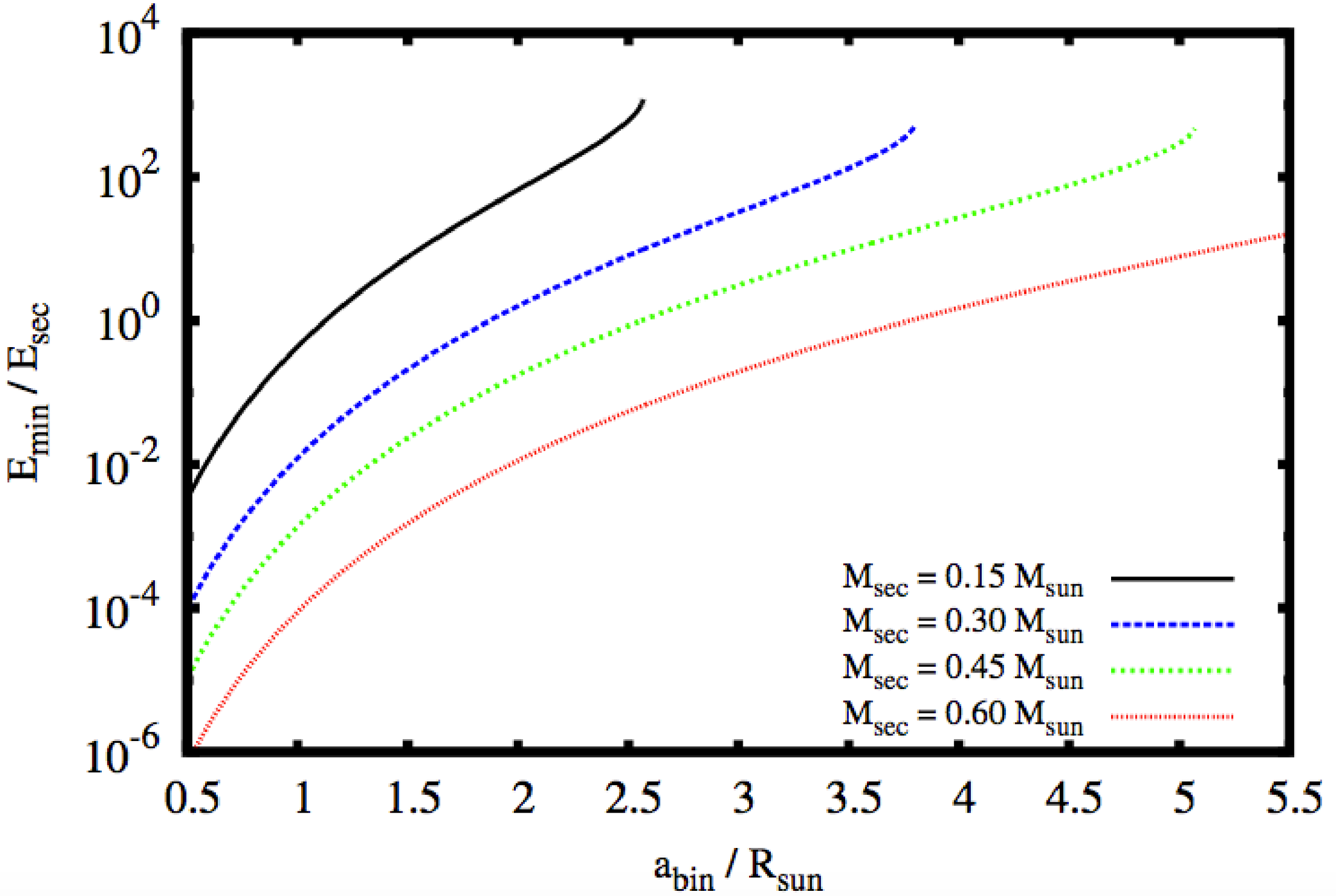

Völschow, Schleicher, Perdelwitz & Banerjee (2016); considering finite-shell model from Brinkworth et al. 2006

Application to observed systems

System	E_{sec}/erg	$\Delta E_{min}/E_{sec}$	$\Delta E/E_{sec}$	$\Delta E/E_{sec}$	$\Delta E/E_{sec}$	$\Delta E_{min}/E_{sec}$	δ_{min}
		Applegate (1992)	Tian et al. (2009)	This paper			
		(see eq. 5)	(see eq. 7)	Const.dens.	Two-zone	Full model	
HS 0705+6700	$2.2 \cdot 10^{39}$	6.7	7.3	3,300	140	140	0.73
HW Vir	$2.0 \cdot 10^{40}$	4.9	6.0	720	108	104	0.72
NN Ser	$2.7 \cdot 10^{39}$	3.2	3.3	1,100	64	64	0.73
NSVS14256825	$8.3 \cdot 10^{38}$	5.3	5.4	3,200	101	102	0.73
NY Vir	$1.4 \cdot 10^{39}$	5.5	5.6	2,800	106	106	0.73
HU Aqr	$1.4 \cdot 10^{40}$	0.10	0.10	240	1.9	1.9	0.732
QS Vir	$3.0 \cdot 10^{40}$	0.039	0.040	170	0.71	0.77	0.71
RR Cae	$5.2 \cdot 10^{39}$	2.8	2.9	560	59	59	0.73
UZ For	$4.1 \cdot 10^{39}$	0.14	0.15	360	2.7	2.7	0.73
DP Leo	$2.9 \cdot 10^{39}$	0.021	0.021	150	0.38	0.38	0.74
V471 Tau	$2.0 \cdot 10^{42}$	0.014	0.014	12	0.26	0.26	0.84
RU Cnc	$5.7 \cdot 10^{43}$	0.074	0.076	1.7	-	-	-
AW Her	$8.5 \cdot 10^{42}$	608	618	270	-	-	-
HR 1099	$3.7 \cdot 10^{43}$	0.21	0.22	10	-	6.7	0.64
BX Dra	$3.5 \cdot 10^{43}$	0.00016	0.00016	0.92	0.0029	0.056	0.52
SZ Psc	$9.9 \cdot 10^{43}$	0.12	0.13	4.7	-	4.84	0.61

Völschow, Schleicher, Perdelwitz & Banerjee (2016)

Modeling the dynamo in a solar-mass star (3 times solar rotation) with the Pencil code

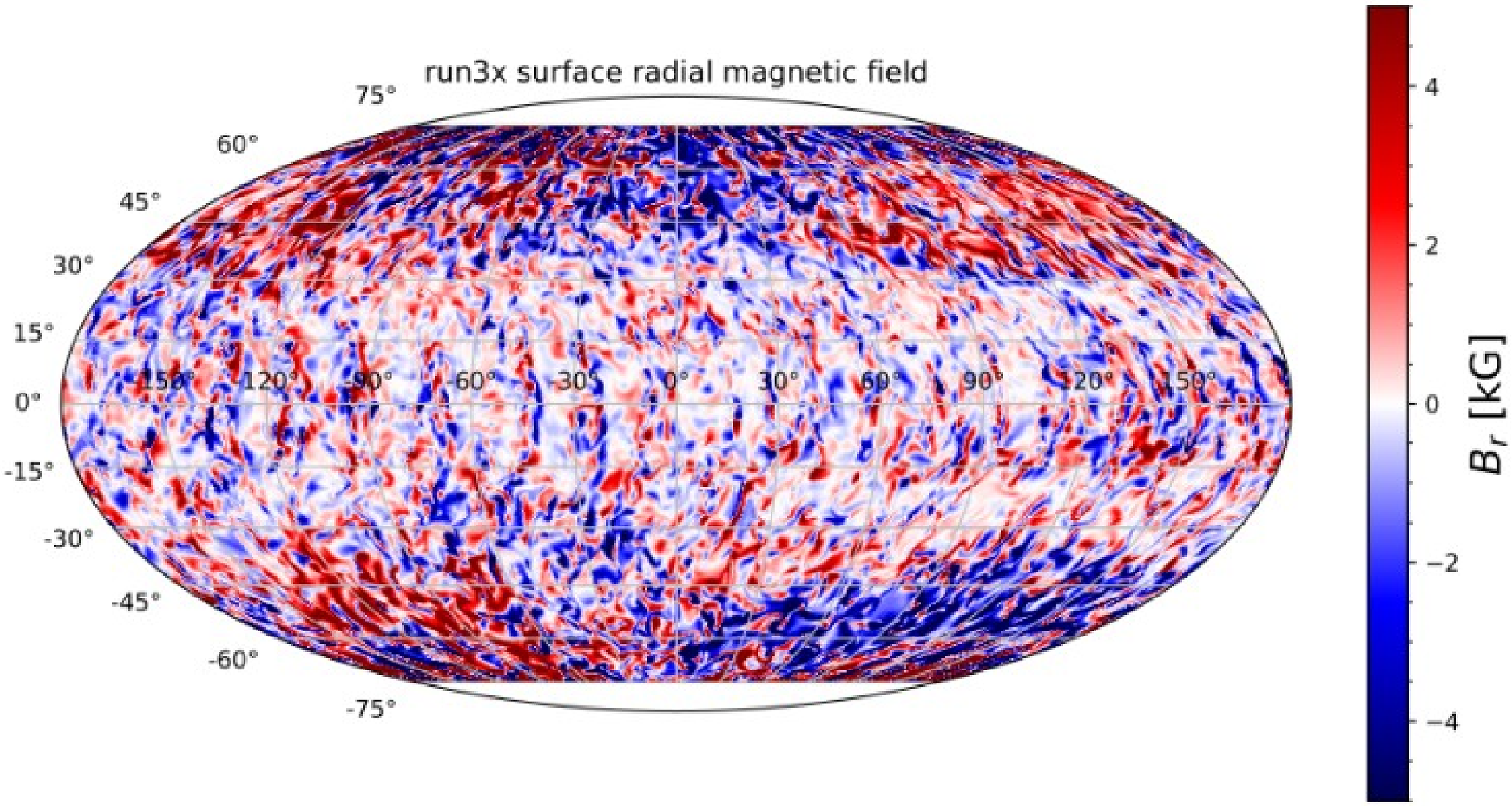

Navarrete, Schleicher et al. (2020)

Evolution of the magnetic field at different depths

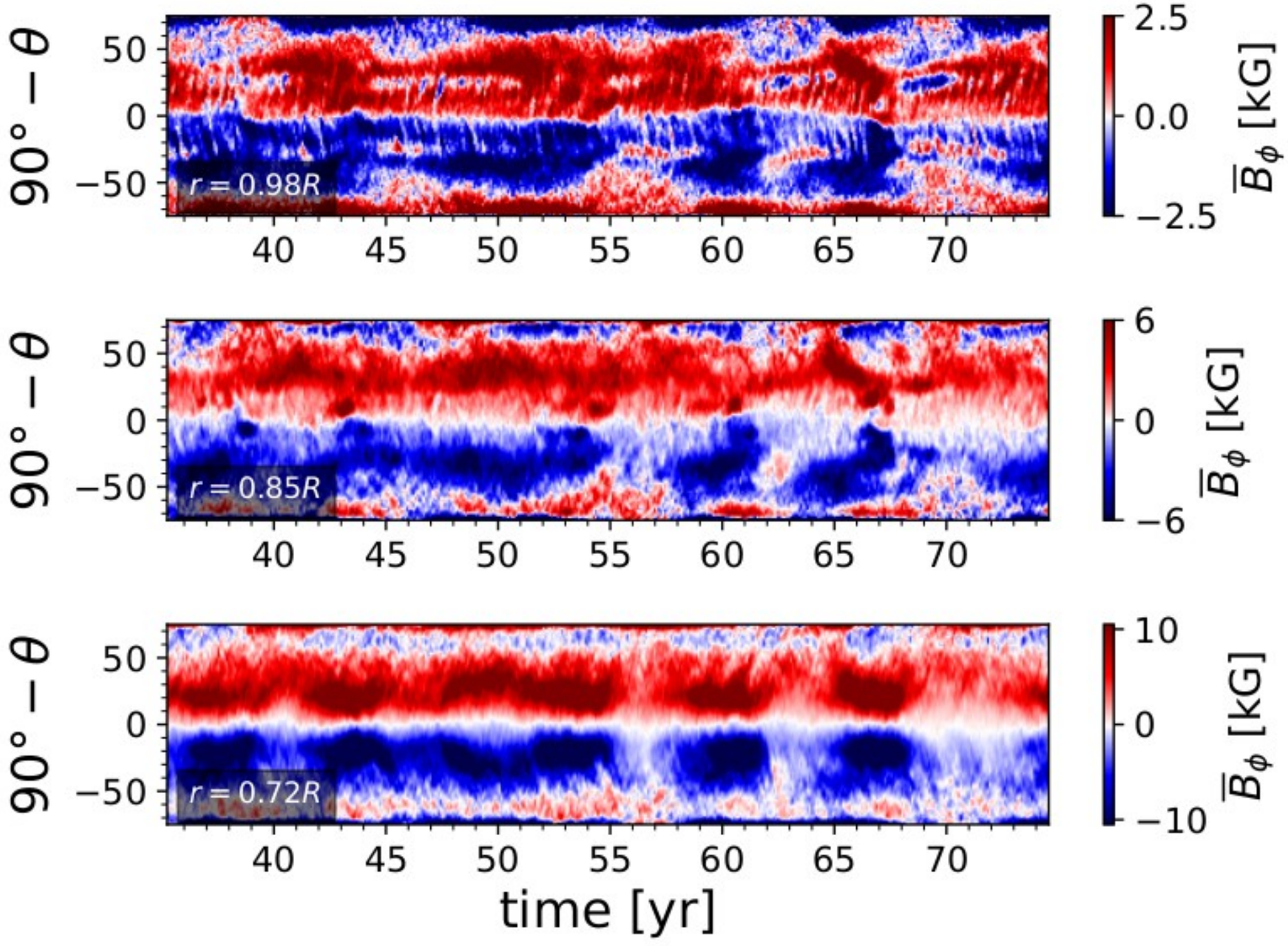

Navarrete, Schleicher et al. (2020)

Correlation of magnetic energy and quadrupole moment

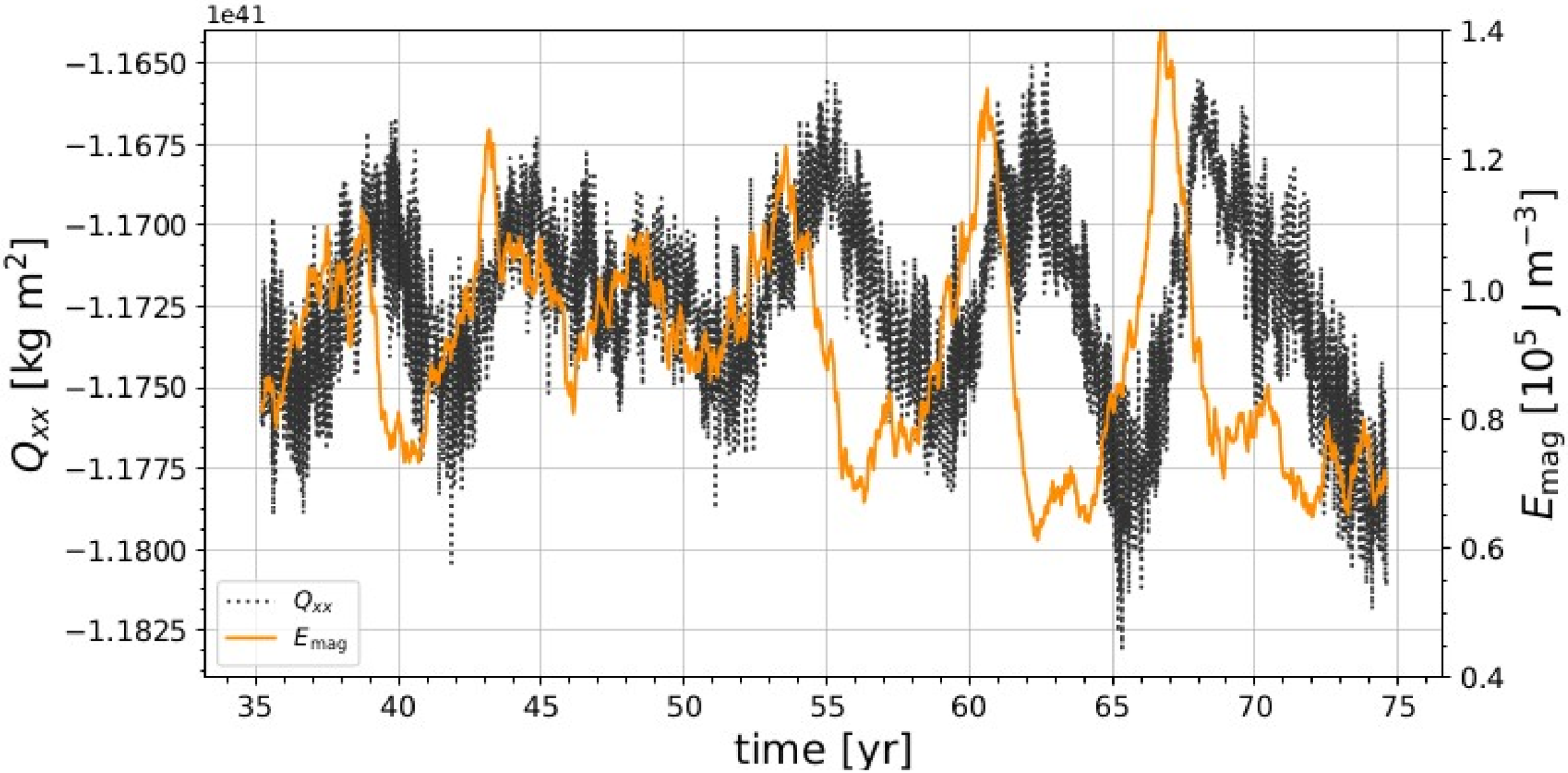

Navarrete, Schleicher et al. (2020)

Spherical harmonic decomposition of the magnetic field components

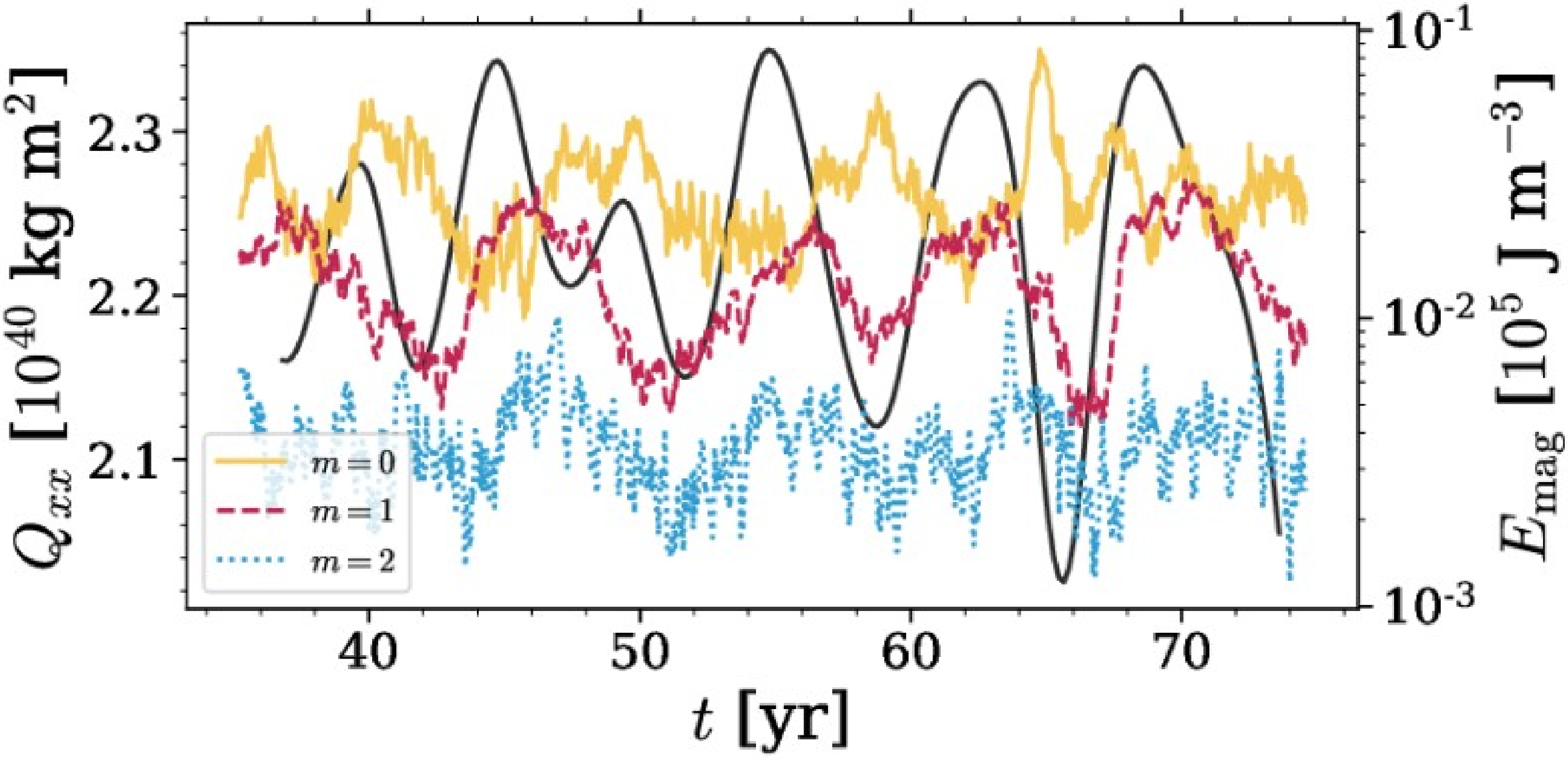

Navarrete et al. (2021)

Quadrupole moment and magnetic energies for system with 30 times solar rotation

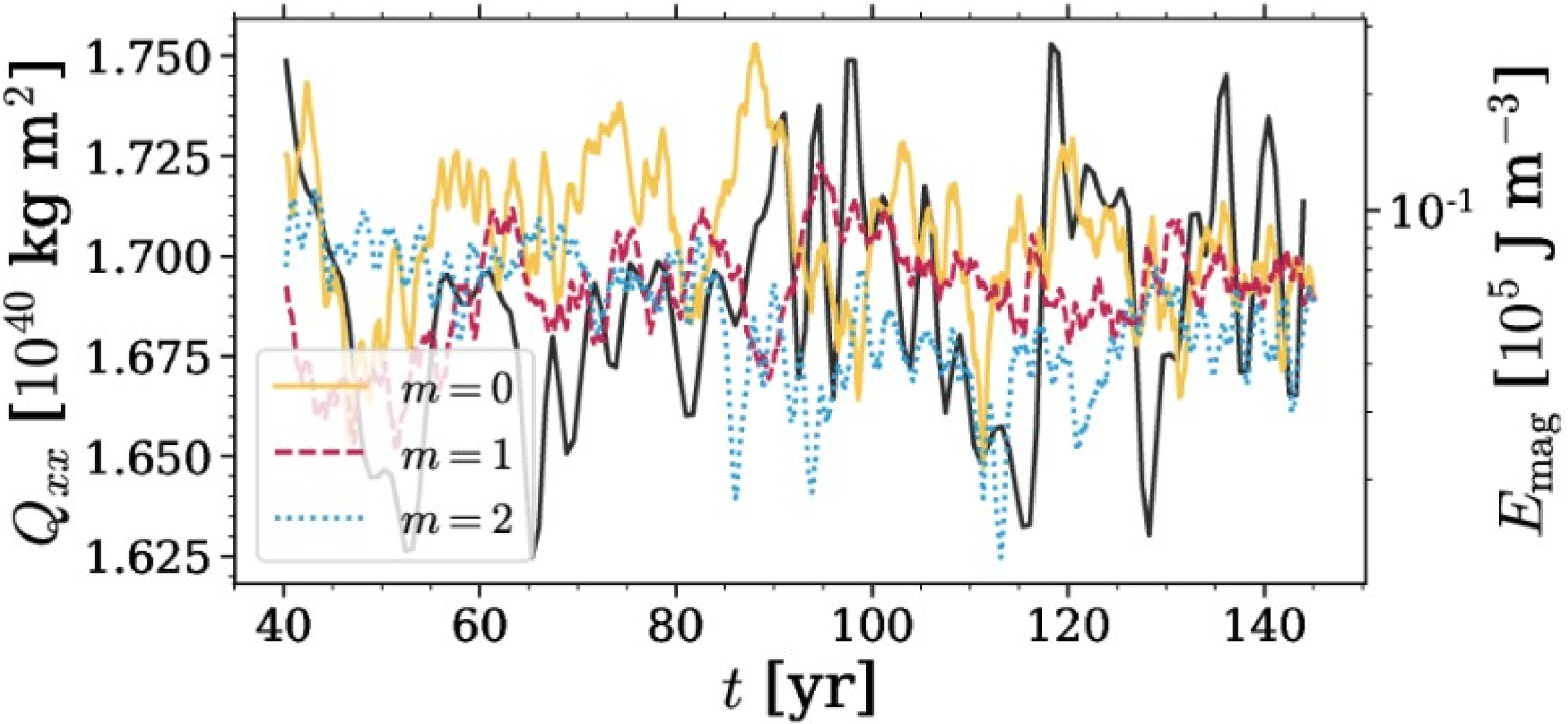

Navarrete et al. (2021)

Implications

The obtained quadrupole moment variations are about two orders of magnitudes too low to explain the observed eclipsing time variations through time-varying changes of the quadrupole moment.

However, Applegate (1989) and Lanza (2020) pointed towards a alternative possibility: the existence of a quasi-permanet quadrupole moment and spin-orbit coupling. The quadrupole moments found in our simulations are indeed sufficient to explain the variations in this scenario.

Navarrete et al. (2021)

Azimuthal dynamo waves in M-dwarfs

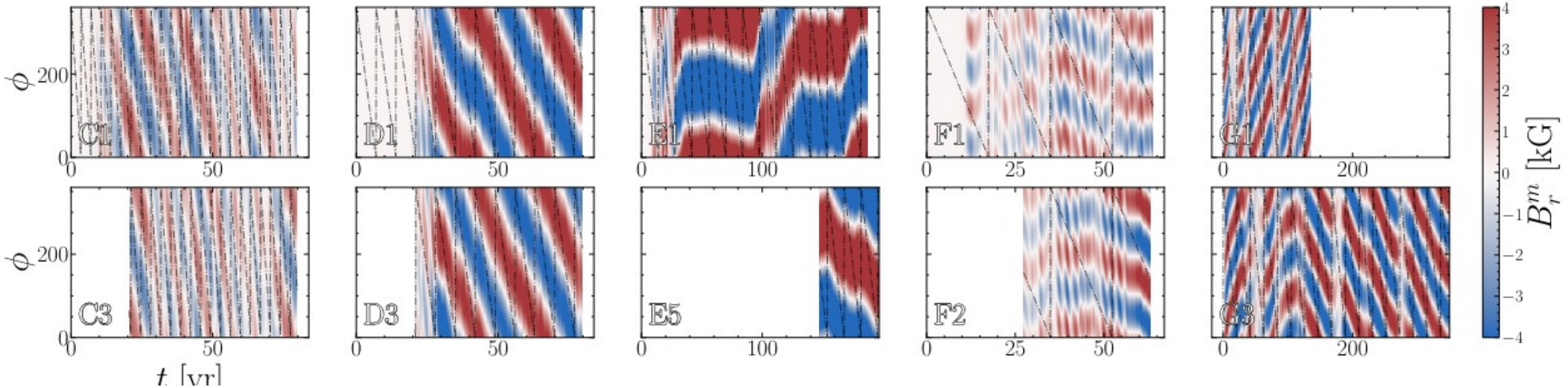

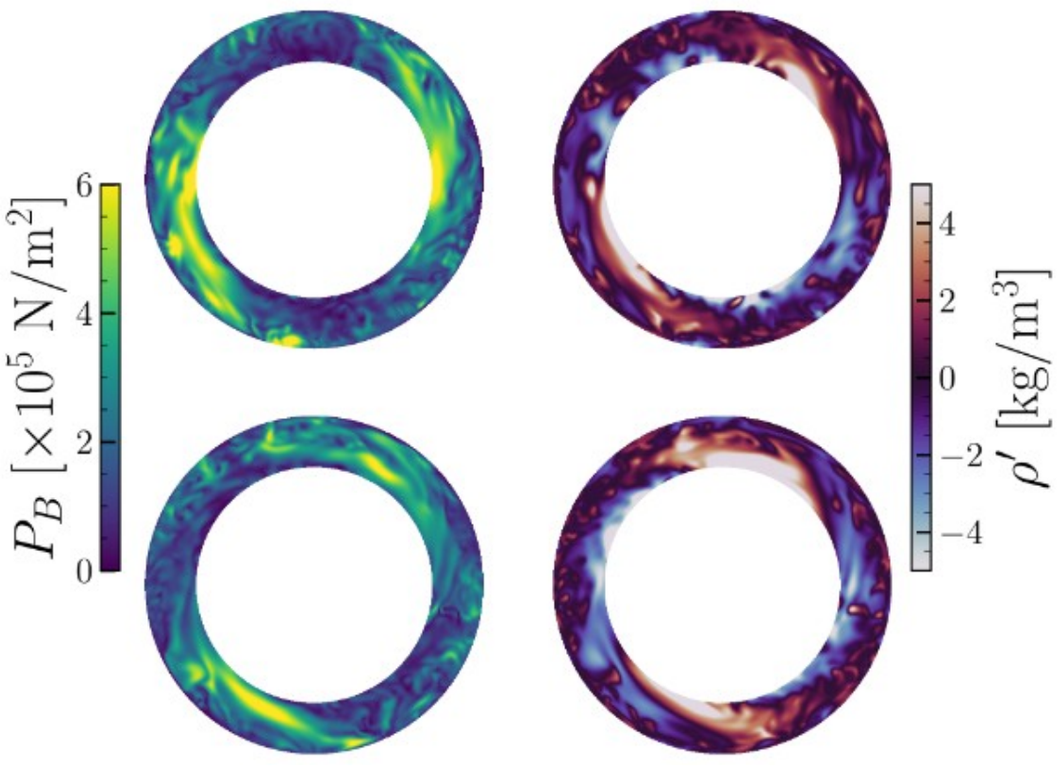

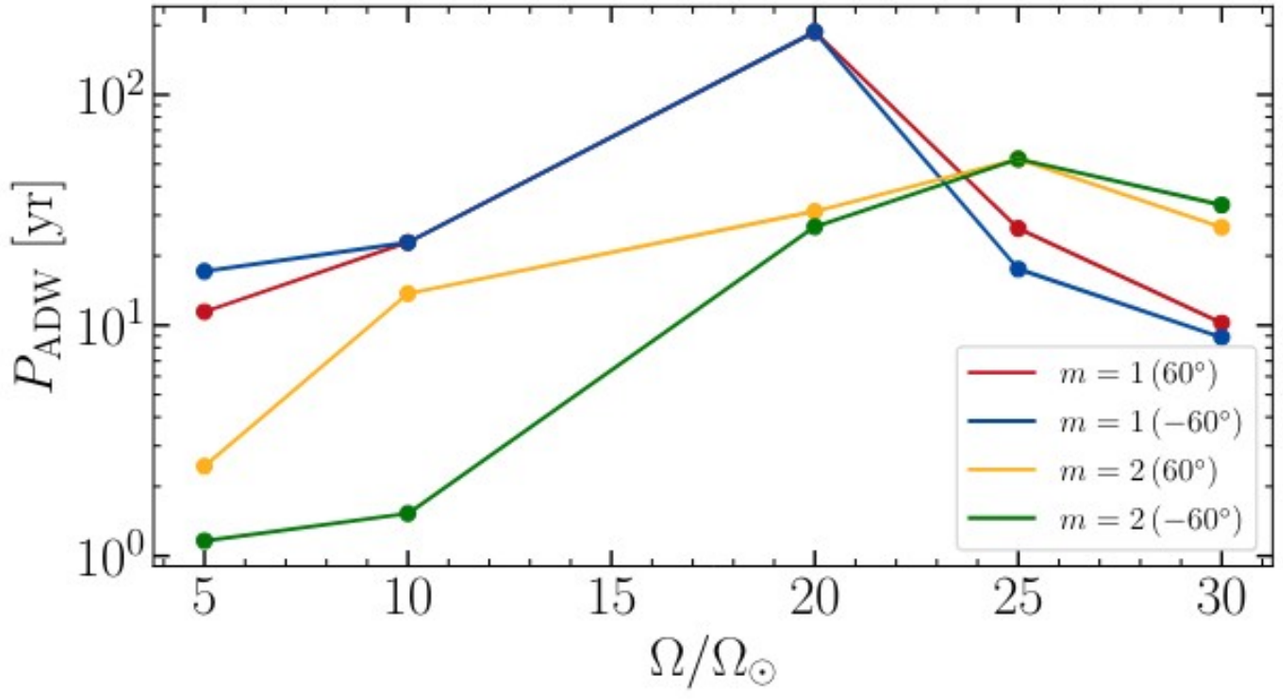

Navarrete et al. (2023); Navarrete et al., in prep.

Eclipsing time variations from azimuthal dynamo waves

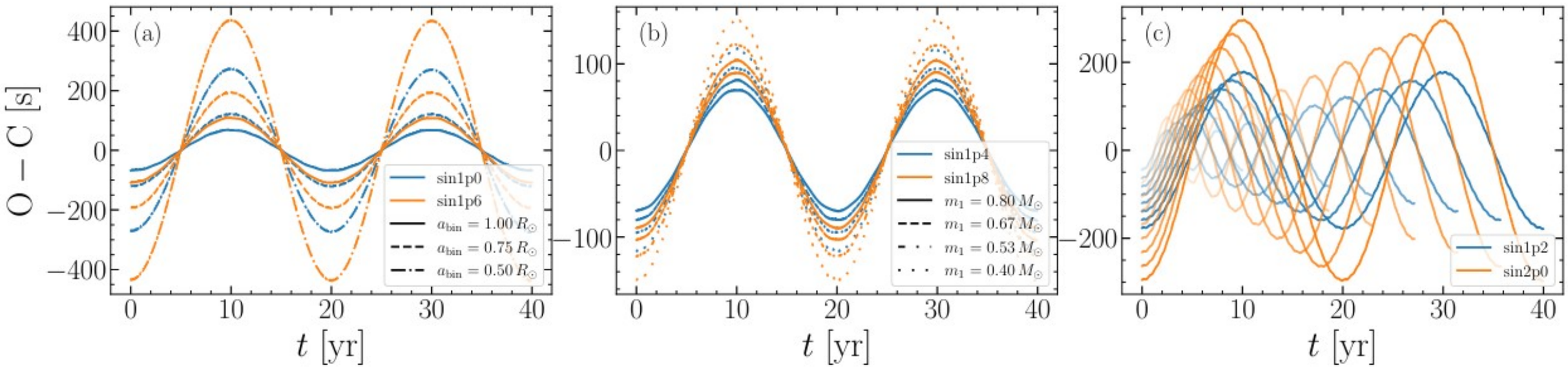

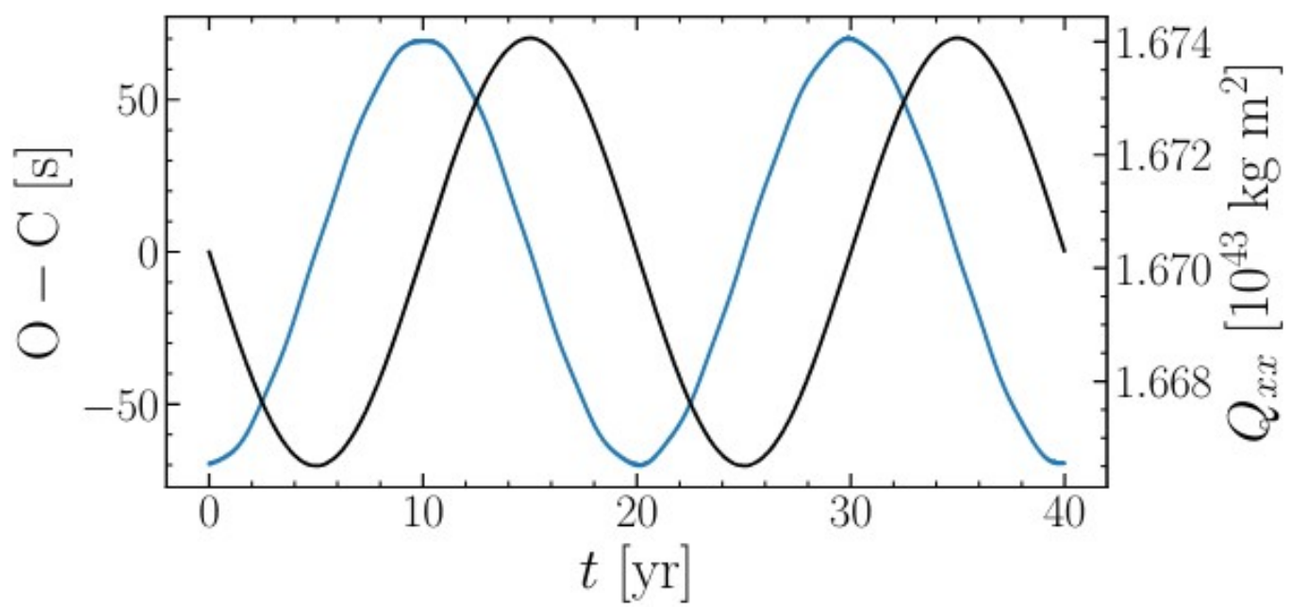

Navarrete et al., in prep.

Implications of time-dependent quadrupole moment

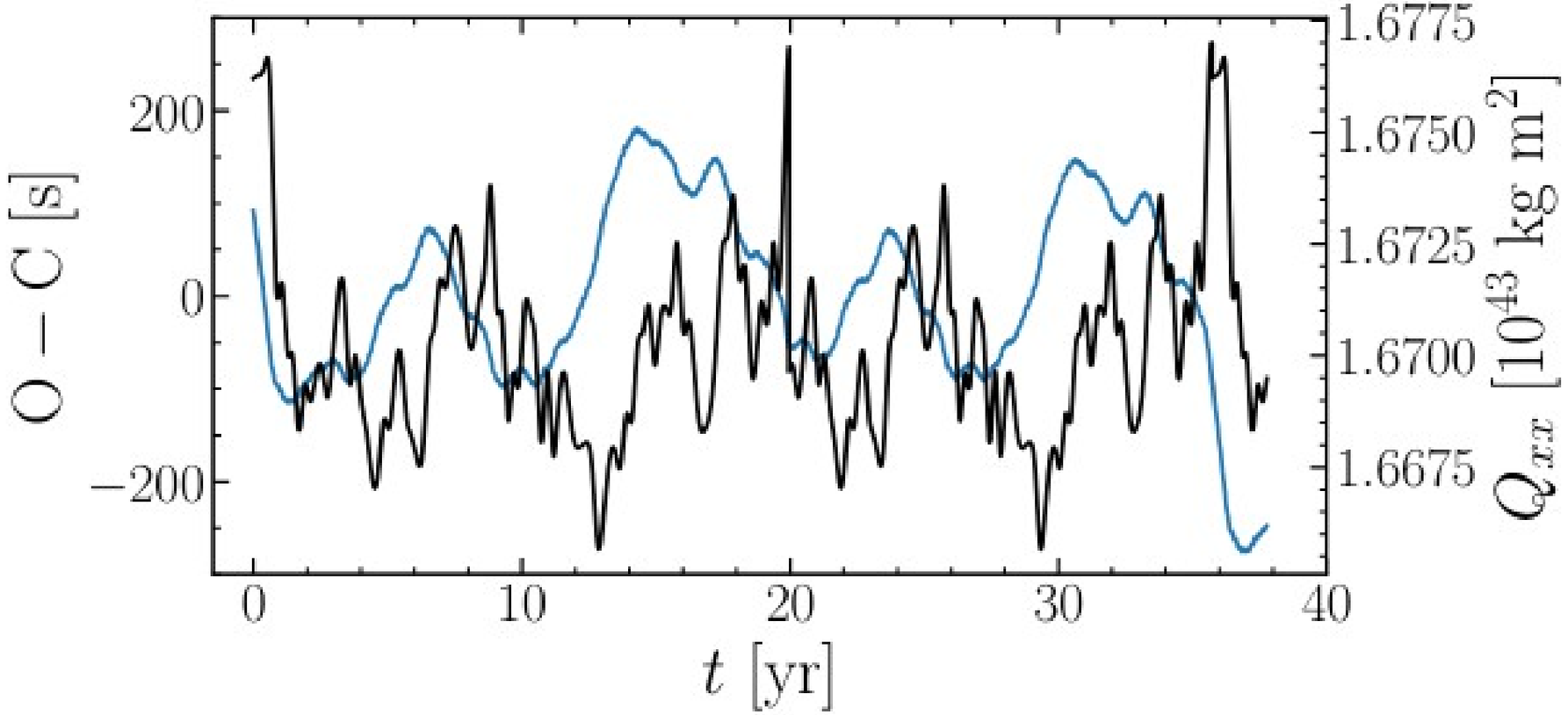

Fig. 8. O − C diagram (blue) for the eclipsing times of a run with a qudrupole moment directly taken from an MHD simulation. The quadrupole moment Q_{xx} is shown in black.

Navarrete et al., in prep.

Summary

Rapid rotation in binary systems may efficiently drive magnetic dynamo processes.

The long period in Double Periodic Variables (DPVs) can be explained as a fixed relation between activity cycle, rotation period and dynamo number (Schleicher & Mennickent 2017).

Dynamo processes were invoked to drive the Applegate mechanism in post-common-envelope systems to explain the observed eclipsing time variations.

For the first time, we have quantified how the stellar quadrupole moment is affected by magnetic activity from 3D simulations. We find that it can explain the eclipsing time variations via spin-orbit coupling (Navarrete et al. 2020, 2021).

Azimuthal dynamo waves could provide a natural explanation for the origin of the eclipsing time variations (Navarrete et al., in prep.).